Eur Biophys J (2002) 31: 207–216
DOI 10.1007/s00249-002-0209-3

ARTICLE

Indira H. Shrivastava · Mark S.P. Sansom

Molecular dynamics simulations and KcsA channel gating

Received: 3 September 2001 / Accepted: 7 January 2002 / Published online: 15 March 2002

Abstract The gating mechanism of a bacterial potassium channel, KcsA, has been investigated via multi-nanosecond molecular dynamic simulations of the channel molecules embedded in a fully solvated palmitoyloleoylphosphatidylcholine bilayer. Four events are seen in which a cation (K^+ or, in one case, Na^+) initially present in the central cavity exits through the intracellular mouth (the presumed gate) of the channel. Whilst in the cavity a cation interacts with the sidechain T107 Oγ atom of one of the subunits prior to its exit from the channel. Secondary structure analysis as a function of time reveals a break in the helicity of one of the M2 helices. This break is expected to lend flexibility to the helices, enabling them to "open" (minimum pore radius >0.13 nm) and "close" (minimum pore radius <0.13 nm) the channel. Fluctuations in the pore radius at the intracellular gate region are of the order of 0.05 nm, with an average radius in the region of the gate of ca. 0.1 nm. However, around the time of exit of a cation, the pore widens to about 0.15 nm. The distances between the Cα atoms of the inner helices M2 reveal a coupled increase and decrease between the opposite pair of helices at about the time of exit of the ion. This suggests a breathing motion of the M2 helices that may form the basis for a gating mechanism.

Keywords Ion channel · Membrane protein · Molecular dynamics · Gating · Potassium ion

I.H. Shrivastava (✉) · M.S.P. Sansom (✉)
Laboratory of Molecular Biophysics,
Department of Biochemistry,
The Rex Richards Building,
University of Oxford, South Parks Road,
Oxford OX1 3QU, UK
E-mail: shrivasi@helix.nih.gov
E-mail: mark@biop.ox.ac.uk
Tel.: +44-1865-275371
Fax: +44-1865-275182

Current address: I.H. Shrivastava
LECB, NIC, Bethesda MSC 5677,
MD 20892-5677, USA

Introduction

Ion channels are integral membrane proteins that play an important role in membrane permeability, enabling rapid (ca. 10^7 ions s^{-1} $channel^{-1}$) passive movements of selected ions across membranes. Excitation and electrical signalling in the nervous system is due to movement of ions through the ionic channels (Hille 1992). These proteins play an essential role in physiology and pathology of a wide variety of cells. Malfunctioning of the ion channels, due to mutations, have been shown to lead to neurological diseases sometimes referred to as "channelopathies" (Ashcroft 2000). Although considerable electrophysiological and related data are available, the molecular mechanisms underlying channel function remain elusive. In particular, we would like to understand the physical bases of ion permeation and selectivity, and of channel gating. The latter topic is the subject of this paper.

The determination of the 0.32 nm resolution X-ray crystal structure of KcsA (Doyle et al. 1998), a bacterial channel from *Streptomyces lividans* (Schrempf et al. 1995), provides an excellent opportunity to understand key aspects of channel functions at a molecular level. This bacterial K^+ channel, which shows sequence similarity to other K channels (Doyle et al. 1998; Schrempf et al. 1995), has been studied from both a structural (Cortes et al. 2001; Jiang and MacKinnon 2000; Perozo et al. 1998, 1999, 2000; Zhou et al. 2001) and functional (Cuello et al. 1998; Heginbotham et al. 1999; Meuser et al. 1999, 2001; Splitt et al. 2000) perspective via a variety of techniques. In particular, studies using a K channel-specific scorpion neurotoxin suggest that KcsA shares many structural features with the pore forming domain of voltage gated (Kv) potassium channels, at least at its extracellular mouth (MacKinnon et al. 1998). Hence investigations on KcsA are expected to help us understand structure/function relations in K channels in general (Biggin et al. 2000). However, one must remain aware of possible differences in some aspects of channel

structure between KcsA and Kv channels (Camino et al. 2000; Minor 2001).

The KcsA molecule is tetrameric, with four-fold symmetry about a central pore axis. Each subunit consists of an outer helix (M1) that is exposed to the membrane and an inner pore-lining helix (M2). M1 and M2 are linked by a 30 amino acid pore (P) region, made up of a turret, which is exposed to the extracellular solvent, a pore helix and the selectivity filter (F) region (Fig. 1A). There is a large (volume ca. 0.8 nm^3, i.e. big enough to hold ca. 27 water molecules) hydrophobic cavity in the centre of the channel, which in the crystal appears to be filled with water molecules plus a single K^+ ion. The four P helices are inclined at an angle of ~45° with respect to the pore axis such that their C-termini point towards the centre of the cavity. This has been suggested to help provide electrostatic stability to a monovalent cation within the cavity (Roux and MacKinnon 1999).

A channel may be regarded as an allosteric protein that responds to a stimulus (e.g. membrane potential change, chemical stimulus or mechanical deformation) by switching its conformation (Hille 1992). This conformational transition of the channel, known as "gating", controls opening and closing of the pore. Early studies on the kinetics of Kv channel blockade by quaternary ions (Armstrong 1971) suggested that both open-channel block and ion-trapping effects are associated with changes at the *intracellular* end of the protein. More recently, structural (Perozo et al. 1998, 1999, 2000; Zhou et al. 2001) and functional (Cortes et al. 2001; Cuello et al. 1998; Heginbotham et al. 1999) studies of KcsA place the gate at the intracellular mouth of this channel. Functional analysis of C-terminal deletion constructs suggests that the C-terminal domain (absent from the X-ray structure) has a modulatory role in pH-dependent gating of KcsA (Cortes et al. 2001). Energetic considerations (Biggin et al. 2001b; Roux et al. 2000) suggest that the narrow intracellular mouth of the KcsA pore forms a hydrophobic barrier to ion permeation that may correspond to the gate. Significantly, a narrow hydrophobic barrier has been suggested to form the gate in bacterial mechanosensitive channels (Sukharev et al. 2001). In voltage gated channels the gate also appears to be at the intracellular mouth of the channel (Camino et al. 2000), although the detailed architecture of this region is likely to differ from that of KcsA owing to the presence of a proline-induced kink in the S6 helix (Shrivastava et al. 2000; Tieleman et al. 2001b), i.e. in the equivalent helix to M2 in KcsA.

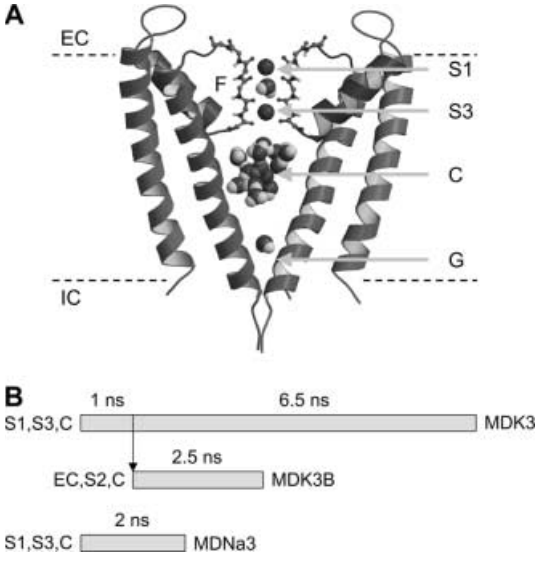

Fig. 1 **A** Diagram of KcsA showing, for clarity, only two of the four subunits. Selected water molecules and K^+ ions are shown. *S1* and *S3* indicate K^+ ions at these two sites within the selectivity filter (*F*), with a water molecule (at S2) in between. There is a further cluster of water molecules surrounding a K^+ ion in the cavity (*C*) and a water molecule close to the intracellular gate (*G*). The *broken horizontal lines* indicate the approximate location of the water/bilayer interface, and *EC* and *IC* indicate the extracellular and intracellular surfaces, respectively. Diagram generated using Molscript (Kraulis 1991) and Raster3D (Merritt and Bacon 1997). **B** Diagram of the simulations discussed in this paper. In simulation MDK3 the initial locations of the three K^+ ions were at S1, S3 and in the cavity (as shown in **A**). The starting configuration of simulation MDK3B derived from a snapshot of MDK3 at 1 ns, with the three K^+ ions at the extracellular mouth of the channel, at S2 and in the cavity, respectively. In simulation MDNa3 the starting configuration was similar to that for MDK3, but with Na^+ ions replacing K^+ ions

In this paper we employ molecular dynamics (MD) simulations to study possible gating mechanisms of KcsA. Simulation studies have already been employed to investigate ion permeation and selectivity mechanisms of KcsA and related K channels (Allen et al. 1999, 2000; Åqvist and Luzhkov 2000; Bernèche and Roux 2000; Biggin et al. 2001b; Capener et al. 2000; Guidoni et al. 1999, 2000; Luzhkov and Åqvist 2000; Ranatunga et al. 2001a, 2001b; Shrivastava and Sansom 2000; reviewed by, for example, Roux et al. 2000; Sansom et al. 2000; Tieleman et al. 2001a). Simulations have also been used to explore the inherent flexibility of certain transmembrane (TM) α-helices in membrane proteins such as channels and receptors (Sansom and Weinstein 2000). In this paper we explore in more detail an event first reported in an earlier paper (Shrivastava and Sansom 2000), namely the structural changes occurring in the KcsA protein prior to the exit of the ion through the intracellular mouth (i.e. the presumed gate region) of the pore.

Methods

Simulation systems

The starting protein structure for the simulations was that as in PDB file 1bl8, modified by addition of "missing" atoms for sidechains not present in the crystal structure, which were added by building in stereochemically preferred conformers. The N- and C-terminal extramembraneous regions (residues 1–22 and 120–160), which are absent in the X-ray structure, were not included in the simulation model. A fully equilibrated palmitoyloleoylphosphatidylcholine (POPC) lipid bilayer (kindly provided by Dr Peter Tieleman) was

used as starting point in which the KcsA protein was inserted. The final simulation system consisted of 243 POPC molecules, 9821 SPC water molecules and 7 Cl^- counter ions, to set the net charge of the system to zero.

The setup of the simulation system was as described elsewhere (Shrivastava and Sansom 2000; Shrivastava et al. 2000). In this paper we will focus on those simulations in which ion exit through the intracellular (IC) "gate" was observed, as summarized in Fig. 1B. Simulation MDK3 is an extension (from ca. 1 ns to ca. 7 ns) of MDK3 in Shrivastava and Sansom (2000). This simulation started from a configuration with two K^+ ions (K1 and K2) in the selectivity filter (at sites S1 and S3) plus a third K^+ ion (K3) located close to the centre of the cavity. Simulation MDK3B originated from the 1 ns "snapshot" of MDK3 [i.e. the end of simulation MDK3 in Shrivastava and Sansom (2000)], at which time K3 had exited the channel and was close to the IC mouth in the "bulk" water. At the same time, K1 had moved to S2 of the filter and K2 to the cavity. At the start of MDK3B this configuration was modified by moving K3 to the extracellular (EC) mouth of the channel. The simulation was run for 2.5 ns. For comparison, we include a third simulation in which ion exit has been observed, namely MDNa3. In the initial configuration of this simulation, three Na^+ ions occupied the same positions similar to the K^+ ions in MDK3. MDNa3 was run for 2 ns. Again, here we focus on the ion exit event. Differences in the behaviour of K^+ and Na^+ ions in the *filter* of KcsA are described in Shrivastava et al. (2002).

Simulation protocol

The simulation protocol was similar to that used in our previous simulations (Capener et al. 2000; Shrivastava and Sansom 2000). The MD simulation package used was GROMACS v1.6 (http://rugmd0.chem.rug.nl/-gmx/gmx.html). Lipid parameters were based on Berger et al. (1997) and Marrink (1998). The lipid-protein interactions used GROMOS parameters and the water model used was SPC (Berendsen et al. 1981), which has been shown to be a reasonable choice for lipid bilayer simulations (Tieleman and Berendsen 1996). A twin range cut-off was used for electrostatic calculations: 1.0 nm for van der Waals and 1.7 nm for electrostatic calculations. Note that the distances between, for example, K1 and K2, or K2 and K3, at the start of the simulation (0.7 nm and 1.0 nm) do not exceed this cutoff. The time step was 2 fs, with the neighbour list updated every 10 steps. The LINCS algorithm (Hess et al. 1997) was used to constrain bond lengths and the simulations were all done under NPT conditions, with a constant pressure of 1 bar in all three directions and a coupling constant of $\tau_p = 1.0$ ps. Water, lipid and proteins were coupled separately to a temperature bath at 300 K with a coupling constant of $\tau_t = 0.1$ ps. The K^+ and Na^+ parameters were as in Straatsma and Berendsen (1988). All the simulations were performed on an 86-node SGI Origin2000. The program DSSP (Kabsch and Sander 1983) was used for analysis of secondary structure. The HOLE program (Smart et al. 1993, 1997) was used to calculate the pore radius profiles and the other analyses was done using GROMACS routines or our own code. Structural diagrams were prepared using Molscript (Kraulis 1991) and Raster3D (Merritt and Bacon 1997).

Results

Cavity ion exit events

In the present work, we are going to focus on ions in the central cavity and their exit from the channel via the IC gate. This can be readily visualized by plotting the coordinate trajectories of the ions, projected onto the pore (z) axis, with $z = 0$ corresponding to the centre of the filter, z = ca. –1.3 nm at the centre of the cavity and z = ca. –2.5 nm at the IC gate. Thus, in simulation MDK3, two ion exit events are seen: one in the first part of the simulation (not shown) at ca. 0.95 ns, when K3 moves from the cavity (C) to the IC region, and one at ca. 6 ns when K2 moves C to IC (Fig. 2A). In MDK3B, ion K2 moves from C to IC at ca. 2.2 ns (Fig. 2B). In MDNa3, Na3 moves from C to IC at ca. 1.3 ns (Fig. 2C). Note that, in both MDK3 and MDK3B, K2 does not exit from the cavity until K3 has (re)entered the selectivity filter. It appears that the presence of two K^+ ions in the filter is correlated with the cavity ion moving "down" the cavity and eventually exiting. The exit of an ion is thus a rare event in these simulations: we only see four exit events in a total of ca. 12 ns of simulation time.

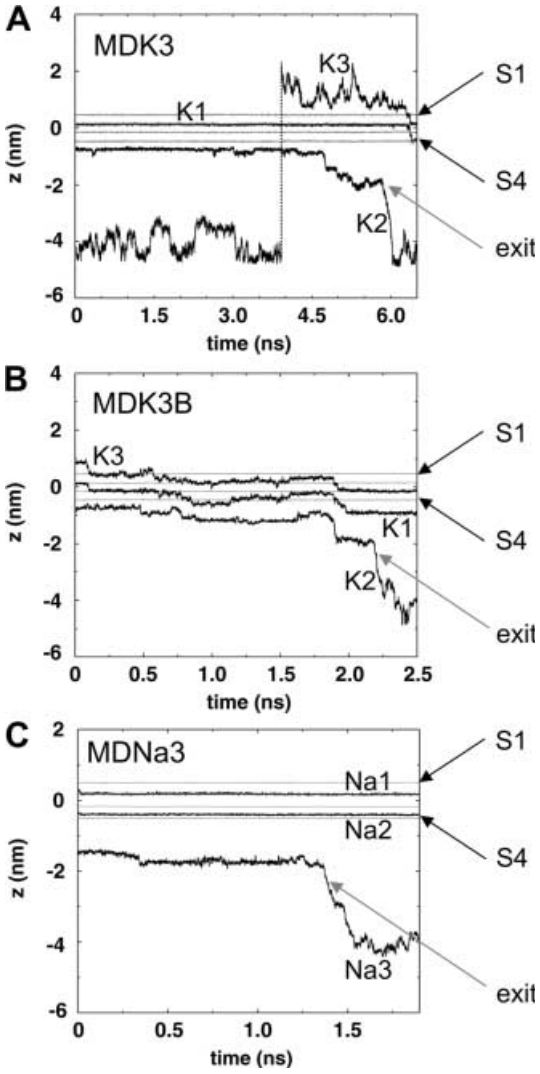

Fig. 2 Trajectories (along the pore z axis) of K^+ or Na^+ ions for simulations: **A** MDK3 (second section, i.e. "6.5 ns" in Fig. 1); **B** MDK3B; and **C** MDNa3. The locations on z of the four filter binding sites (S1–S4) are indicated by *thin horizontal lines*. The intracellular gate of the channel is at z = ca. –2 nm; the centre of the filter is at z = ca. 0 nm. The *arrows* labelled "*exit*" indicate the time at which the ion exits from the cavity through the intracellular gate. The *dotted vertical line* for ion K3 in MDK3 corresponds to the movement of this ion across a periodic boundary at t = ca. 4 ns (see text)

Of course, this small number of events does not permit statistical analysis. However, we note in passing that in a simulation of 7.6 ns duration (MDK3) we do not see a single ion move all the way through the channel. This puts a lower bound of ca. 10 ns on the mean passage time of an ion, which would correspond to a single channel conductance of ca. 160 pS at 100 mV, compared with estimates of ca. 100 pS for the conductance of KcsA (Heginbotham et al. 1999; Meuser et al. 1999; Schrempf et al. 1995). This reassures us that the timescale of motions in our simulations is comparable to that observed experimentally. Of course, we do not have an external applied voltage in our simulations.

Protein dynamics

We will now examine how the structural dynamics of the protein may be related to the IC "gate" through which the exiting K^+ ion moves. Experimentally, the temperature factors of the atoms in the crystal structure provide a measure of the dynamic mobility and/or static disorder of the different regions of the protein. From the temperature factors of the Cα atoms of KcsA crystal structure, it seems that the IC ends of the helices and the "turret" region (i.e. the EC loop between the M1 helix and the P helix) are more flexible than the transmembrane core of the protein (Doyle et al. 1998), although the modest resolution of the structure warns against over-interpretation of these data. A similar overall pattern is seen in the simulation if one plots the root mean square fluctuation (RMSF) from its time-averaged position of each Cα atoms versus the residue number (data not shown). This overall pattern is conserved between the different simulations. Perhaps a more informative way of displaying the results of this analysis is to plot the RMSF of each Cα atom versus its mean z coordinate (Fig. 3). Within the transmembrane (TM) region of KcsA this reveals a "gradient" in overall protein mobility from the EC (lower mobility, Cα RMSF ca. 0.05 nm) to the IC (higher mobility, Cα RMSF ca. 0.1 nm) end of the molecule. A similar pattern was observed by Bernèche and Roux (2000) in their simulations of KcsA.

A more detailed analysis of structural fluctuations in the protein may be obtained via analysis of time-dependent changes in local secondary structure. As expected, there are considerable fluctuations in local secondary structure in the turret loop region and at the IC ends of the TM helices in all the simulations. The M1 and P helices retain their secondary structure undistorted throughout the simulations. The helicity of all but one of the M2s is also maintained throughout all the simulations. However, a break in the helicity of one of the M2s is seen in all of the simulations, close to residue T107 (Fig. 4). This break is seen fairly early on in the simulation for MDK3 (at around 0.6 ns of the first segment of the simulation) in M2 of subunit A and is then maintained throughout this simulation, as well as MDK3B (which is essentially an extension of the first 1 ns of MDK3). In MDNA3, the break in helicity occurs at about 0.6 ps in the M2 helix of subunit B. It is interesting to note that the break in helicity is associated with residue T107, which seems to be involved in interactions with the ion in the cavity (see below). The increase in flexibility resulting from the local loss of secondary structure may be associated with the opening of the IC gate.

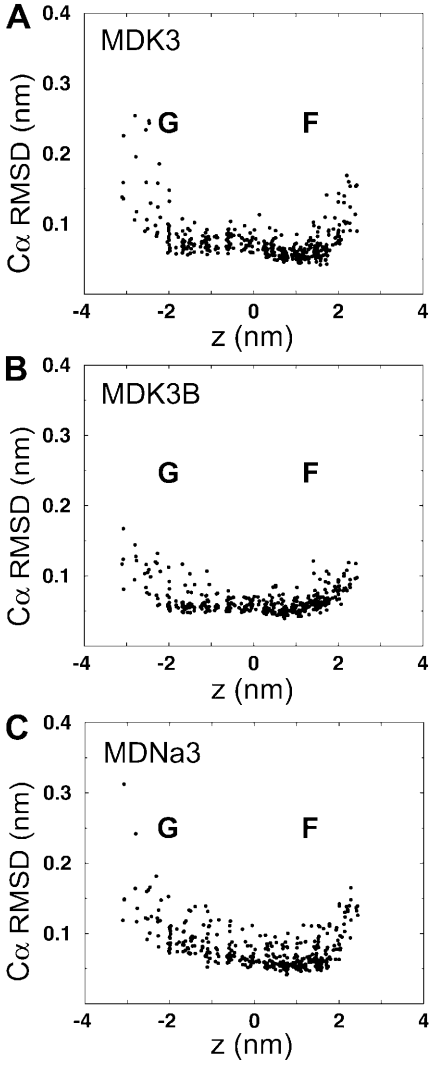

Fig. 3 Root mean square fluctuations (RMSF) versus the z coordinate of the Cα atoms for the three simulations: **A** MDK3; **B** MDK3B; and **C** MDNa3. The gate (*G*) and filter (*F*) regions are denoted in the figure

Site-directed spin labelling and electron paramagnetic resonance (EPR) spectroscopy experiments on the gating in KcsA (Perozo et al. 1998, 1999) suggest that a widening of the pore associated with the gating mechanism is brought about via movement of the M2 helices. From the analysis of secondary structure, we might suspect that this is associated with re-packing of the C-terminal (IC) segments of the M2 helices. To explore this further, the distance between the Cα atoms of the M1 and M2 helices as a function of time was analysed. The inter-M1 helix distances were more or less constant

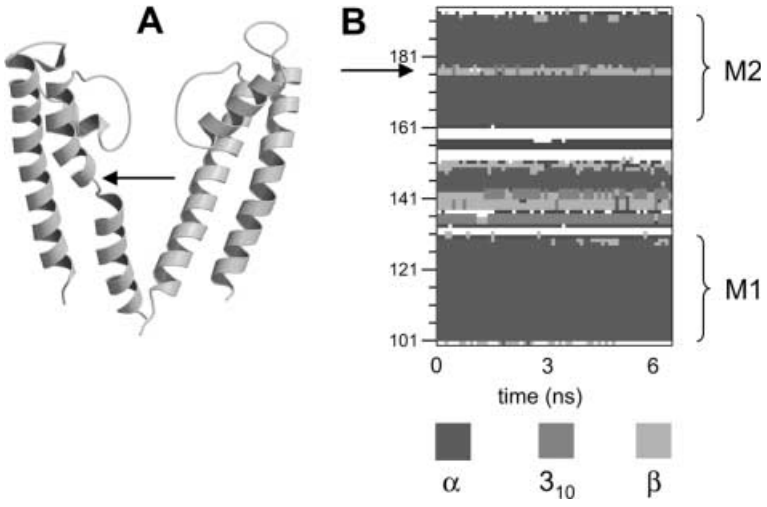

Fig. 4 **A** Snapshot (at t = ca. 1 ns) from simulation MDK3 showing local distortion (*arrow*) of one of the four M2 helices. **B** Secondary structure versus time (for the latter 6.5 ns) of the distorted subunit from simulation MDK3. α-Helical regions are indicated *by dark grey*; the local loss of α-helicity in M2 is indicated by an *arrow*

throughout the simulation. The M2 helix was split into three segments, each consisting of 10 Cα atoms: an N-terminal segment (R89 to A98), a middle segment (G99 to A108) and a C-terminal segment (A109 to G118). The N-terminal segment, close to the selectivity filter, did not show any significant changes in the distances between the opposite pair of helices as a function of time. In contrast, the C-terminal segments, exposed to the IC "bulk" water, showed considerable fluctuations in inter-segment distances. However, these motions do not appear to be correlated with the exit of an ion. The middle segment showed a synchronous change in the distances between the two opposite pairs of helices at around the time of exit of an ion from the channel. Two diagonally opposite helices move closer together (albeit by a small distance, ca. 0.15 nm) whilst the other pair move apart by roughly the same distance simultaneously. The changes in the interhelix distances are of the same magnitude as changes in the pore radius profiles (see below) at around the same time.

Changes in pore dimensions

The ionic radius of K^+ is 0.133 nm (Hille 1992). Thus, in order for a K^+ ion to exit from the channel pore, the radius of the channel pore should be greater than 0.133 nm. If one examines the pore-radius profile of the X-ray structure of KcsA, then in the vicinity of the IC gate the radius is ca. 1 nm (Fig. 5A). Furthermore, the sidechains lining the pore in this region (e.g. V115) are mainly hydrophobic, thus presenting an energetic barrier to a K^+ ion leaving (or entering) the channel. However, this calculation is based upon a single (crystal) conformation of the protein. One may also calculate pore-radius profiles averaged over the entire duration of a simulation, providing an overall measure of the pore radius but taking into account dynamic fluctuations in structure. Doing this for simulations MDK3 (Fig. 5B) and MDK3B (Fig. 5C) reveals that although the pore radius in the gate region fluctuates (SD ca. 0.04 nm), the average value is still ca. 0.1 nm. Thus, on average during each simulation as a whole the gate is closed.

However, transient changes in the pore-radius profiles *are* seen during the simulations, associated with ion exit from the cavity. This is evident if one calculates pore-radius profiles just for the period of the simulation around the time of a cation exit event (Fig. 6A, B). In simulation MDK3, the first opening of the pore is seen at around 0.9 ns in the first segment of the simulation, and is maintained for about 0.1 ns, after which it again closes (Shrivastava and Sansom 2000). Similar transient openings are also seen in simulations MDK3B and MDNa3. The pore radius increases from 0.1 nm to ca. 0.2 nm. In the later stages of the MDK3 simulation (ca. 6 ns) the pore radius is ca. 0.15 to 0.25 nm, suggesting that the channel is truly open. When the ion exits from the channel at ca. 6 ns, the radius increases to ca. 0.3 nm (Fig. 6C). Thus there seems to be "opening" and "closing" of the IC gate associated with the exit of a cation. The minimum pore radius in the IC gate region was monitored versus time, and compared with the minimum radius in the filter region. In all three simulations the minimum radius in the filter region did not show large fluctuations with respect to time, staying constant at ca. 0.1 nm in the two K^+ simulations and ca. 0.05 nm in simulation MDNa3 [the difference between K^+ and Na^+ corresponds to constriction of the filter in the presence of the smaller ion; see Shrivastava et al. (2002) for a detailed analysis]. In contrast, the minimum in the pore radius in the IC gate region varied from ca. 0.07 nm and ca. 0.2 nm as a function of time. Visualization of the internal surface of the pore (Fig. 6C) shows a considerable widening of the pore (almost 0.3 nm) at the intracellular gate, and a degree of distortion of the central cavity from approximate spherical symmetry. A similar widening of the pore is seen in the MDNa3 simulation, with the pore radius increasing to ca 0.25 nm. Thus, it is evident that the structural fluctuations observed during these simulations can induce a functional opening of the IC gate of the channel.

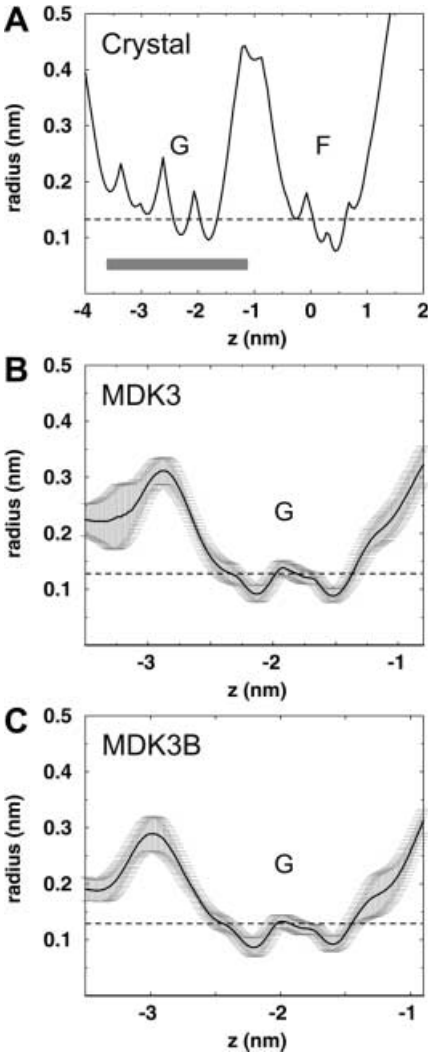

Fig. 5 **A** Pore radius profile [evaluated using HOLE (Smart et al. 1993, 1997)] of the X-ray crystal structure of KcsA, showing the pore radius as a function of position along the *z* axis. The *horizontal broken line* indicates the radius (0.133 nm) of a K^+ ion, and the *grey bar* indicates the location of the intracellular gate (*G*) region. **B**, **C** Average (±SD) pore radius profiles for the gate region for simulations MDK3 (**B**) and MDK3 (**C**). The averages were calculated from snapshots saved every 50 ps throughout the whole simulation, and the *horizontal broken lines* indicate the radius (0.133 nm) of a K^+ ion

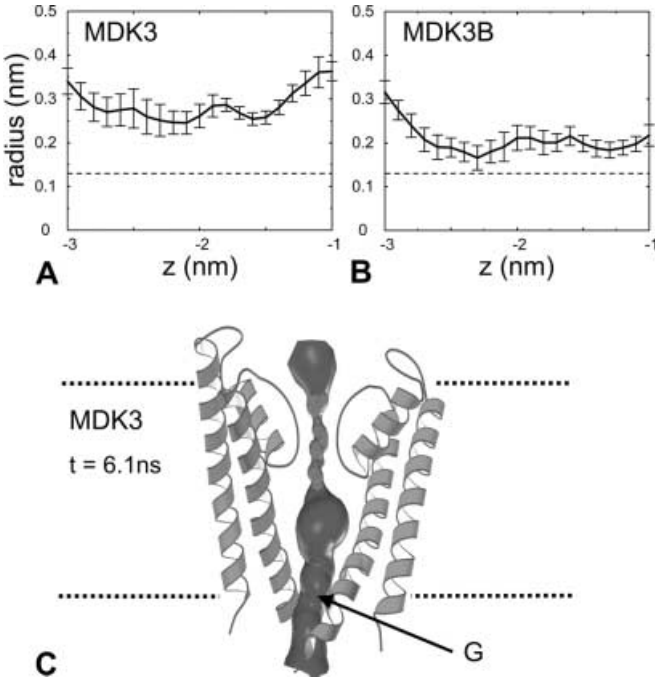

Fig. 6 **A** Average (±SD) pore radius profiles for the gate region for simulation MDK3 calculated from snapshots saved every 50 ps during the period 5.1–6.1 ns (i.e. around the exit of K2; see Fig. 2A). **B** Average (±SD) pore radius profiles for the gate region for simulation MDK3B calculated from snapshots saved every 50 ps during the period 1.75–2.25 ns (i.e. around the exit of K2; see Fig. 2B). **C** Solid surface representation of the pore lining (calculated using HOLE) for simulation MDK3 at 6.1 ns, just after the ion has exited from the pore. The surface is colour coded: radius <0.06 nm, *mid-grey*; radius 0.06–0.115 nm, *pale grey*; radius >0.115 nm, *dark grey*. The pore expansion in the gate region (*G*) is indicated by the *arrow*. For clarity, only two of the four subunits are shown

Ion-protein and ion-water interactions

Having established that the protein conformation changes to permit exit of an ion from the cavity, it is of interest to examine the interactions of that ion with the protein and/or with water molecules before, during and after the exit event. Whilst in the cavity, the ion interacts with mainly a first solvation shell of water molecules (see below), and also with one or more sidechains of the only polar residue lining the cavity, namely T107. This was first reported in the preliminary MDK3 simulation (Shrivastava and Sansom 2000), and here is seen in all three simulations (Fig. 7). During the early stages of MDK3 (0–1 ns), ion K3 interacts with the Oγ atoms of two T107 sidechains until the ion starts to exit. At a later stage in MDK3 (5–6 ns) the interaction of K2 (just prior to its exit through the IC gate) alternates between interactions with three of the four T107 sidechains, though the interaction is somewhat "looser" here owing to the widening of the pore. In MDK3B the interaction alternates between two of the four T107 sidechains. In MDNa3 the ion is initially closely associated with one T107 Oγ for about 0.7 ps, then it seems to sit in the centre of the ring of the four T107 Oγ atoms, before it finally exits from the pore channel at ca. 1.5 ns. Thus, in all of these simulations the T107 residue seems to provide an interaction site for the cation within the largely hydrophobic cavity.

While the ion is exiting from the channel, it cannot interact favourably with any of the protein siechains lining the intracellular gate, since these are all hydrophobic. Instead, all of the interactions of the ion are with water molecules in the cavity water or the "bulk" water outside the channel. One can gain some comparative insights into the nature of cation/water interactions by examining the radial distribution function, $g_{OM}(r)$, of the water oxygen atoms with an ion before and after exit

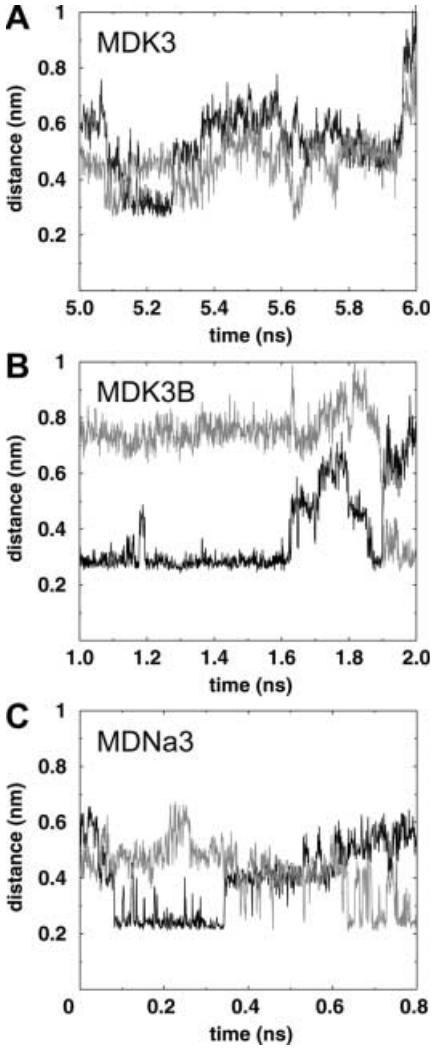

Fig. 7 The distance of the sidechain oxygen, Oγ, of the cavity lining residue, T107, and the cation in the cavity as a function of time for simulations **A** MDK3 from 5 to 6 ns; **B** MDK3B from 1 to 2 ns; and **C** MDNa3 from 0.0 to 0.8 ns. The distances are given for just two of the four T107 residues shown (for clarity)

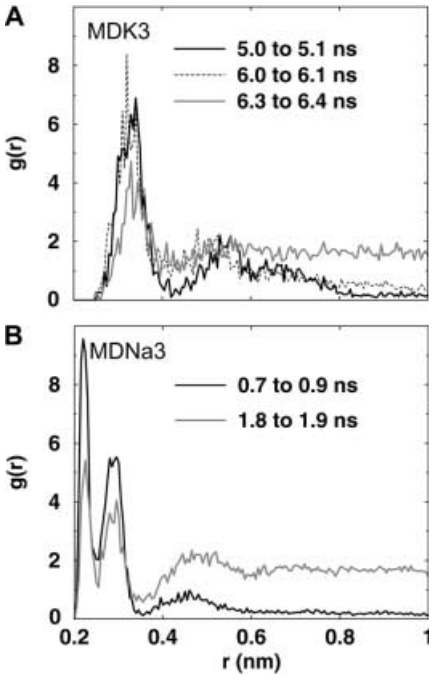

Fig. 8 Radial distribution functions of water around the "cavity" cation before and after its exit from the pore for simulations **A** MKD3 and **B** MDNa3

(Fig. 8). In general, this shows two peaks at $r = $ ca. 0.33 nm and $r = ca.$ 0.55 nm for K^+ (compared with 0.28 and 0.50 nm for Na^+). However, there is a clear time evolution of the $g_{OM}(r)$ as an ion exits. Thus, whilst an ion is within the cavity, both a first and second peak are evident, whereas when an ion is leaving the cavity, and after it has exited, the second peak is less clear and the $g_{OM}(r)$ is significantly > 0 out to at least 1 nm. This suggests that even when the ion is exiting through the narrow (radius < 0.3 nm) hydrophobic pore it continues to interact with water molecules and can start to "feel" waters beyond its first hydration shell.

Examination of "snapshots" of an ion before, during and after exiting from the channel reveals two sets of water molecules around the ion. One set, consisting of 4–5 water molecules, is within a distance of ca. 0.3 nm of the K^+ ion; the other set, consisting of ca. 5–6 water molecules, is at a distance of greater than 0.5 nm, consistent with the quantitative analysis just presented. Thus it seems that the K^+ ion is incompletely hydrated as it exits from the channel. The water molecules that interact with the ion during its exit are mainly the water molecules that have entered the pore from the intracellular end.

Discussion

Possible biological implications

In this study we see that relatively small fluctuations in the conformation of one of the M2 helices of KcsA may result in transient expansion of the intracellular mouth of the channel, enabling a cation to exit from the central cavity. Given the experimental evidence (Cortes et al. 2001; Perozo et al. 1998, 1999, 2000) that suggests the gate of the KcsA channel is primarily located at the intracellular mouth, it is tempting to identify the ion exit events we observe in our simulations with true, physiological gating of the channel. However, the question remains whether the transient openings we observe in our simulation correspond to the same degree of conformational change needed for "full" gating of the channel. One must remember that multiple conductance levels have been reported for KcsA channels (Meuser et al. 1999; Schrempf et al. 1995) and so it is possible that the "open" conformations of KcsA seen in our simulations may correspond to incomplete openings (i.e. sub-conductance levels) of the channel. We note that a correspondence between sub-conductance levels and

incomplete conformational transitions has been suggested for the bacterial mechanosensitive channel MscL (Biggin and Sansom 2001; Sukharev et al. 2001). However, regardless of these considerations, our simulations offer proof of principle that a modest (ca. 0.05 nm) increase in the radius of the hydrophobic intracellular mouth region of KcsA is sufficient to at least partially open the channel gate. This is in agreement with recent theoretical studies of channel gating by control of the radius and hydrophobicity of a narrow pore (Beckstein et al. 2001).

Methodological limitations

It is important to consider the possible limitations of our simulation methodology. Perhaps the main limitation is the relatively short duration of the simulations. Although the current simulations (7.5 ns in one case) are nearly an order of magnitude longer than those previously reported (Shrivastava and Sansom 2000), they still fall well short of even the fastest events (ca. 10 μs) that may be observed via electrophysiology. Thus, it will be necessary to employ a hierarchy of simulation approaches (Sansom et al. 2000), possibly involving Brownian dynamics simulations (Bek and Jakobsson 1994; Chung et al. 1999; Im et al. 2000; Schirmer and Phale 1999; Schnitzer et al. 2000), in order to fully span the gap between structure and physiology.

Other limitations concern the way in which the long-range properties of the simulation system are treated. We have used (relatively long) cutoffs rather than, for example, PME methods (Darden et al. 1993) to approximate long-range electostatic interactions. This is open to some criticism. However, PME methods are not without artefacts (Hunenberger and McCammon 1999; Weber et al. 2000). Furthermore, comparisons of PME and cutoff methods for a related channel model do not suggest any major differences in simulation behaviour (Capener and Sansom 2002). This aspect merits further investigation. Treatment of long-range properties may also explain why we observe exit of ions through the gate but not entry. A single cation in a cavity volume of ca. 1 nm^3 corresponds to a local "concentration" of ca. 1.5 M K^+. The "bulk" solution contains seven Cl^- counterions in a volume of ca. 300 nm^3, corresponding to a local "concentration" of ca. 40 mM Cl^-. Thus one might expect to see a net exit of cations from the cavity when the gate is open. This could be explored more fully by having more ions in the system, plus trying to include a representation of the TM electrochemical potential in the simulations, although the latter is non-trivial (Roux 1999). A further limitation is the relatively small size of bilayer used in the simulation (< 250 POPC molecules). Simulations of large bilayers (Lindahl and Edholm 2000) have revealed mesoscopic undulations in bilayer structure that could conceivably be coupled to channel gating conformational transitions.

Future directions

In summary, our simulations reveal a transient gating motion of KcsA channels that is sufficient to permit exit of ions from the central cavity. This suggests that channel gating may not necessarily involve large concerted motions of the channel subunits in order to lower the energetic barrier to ion entry/exit. However, in order to form a more stable (i.e. longer lived) open state, more substantial conformational changes may be needed. The challenge for the future is to develop simulation and modelling methodologies, possibly involving non-equilibrium simulation methods (Biggin et al. 2001a), that enable us to explore such conformations in more detail.

Acknowledgements This work was supported by grants from The Wellcome Trust and additional computational time was provided by the Oxford Supercomputing Centre. Our thanks to our colleagues for help and discussions.

References

Allen TW, Kuyucak S, Chung SH (1999) Molecular dynamics study of the KcsA potassium channel. Biophys J 77:2502–2516

Allen TW, Bliznyuk A, Rendell AP, Kuyucak S, Chung SH (2000) The potassium channel: structure, selectivity and diffusion. J Chem Phys 112:8191–8204

Åqvist J, Luzhkov V (2000) Ion permeation mechanism of the potassium channel. Nature 404:881–884

Armstrong CM (1971) Interaction of tetraethylammonium ion derivatives with the potassium channels of giant axon. J Gen Physiol 58:413–437

Ashcroft FM (2000) Ion channels and disease. Academic Press, San Diego

Beckstein O, Biggin PC, Sansom MSP (2001) A hydrophobic gating mechanism for nanopores. J Phys Chem B 105:12902–12905

Bek S, Jakobsson E (1994) Brownian dynamics study of a multiply-occupied cation channel – application to understanding permeation in potassium channels. Biophys J 66:1028–1038

Berendsen HJC, Postma JPM, Gunsteren WF van, Hermans J (1981) Intermolecular forces. Reidel, Dordrecht

Berger O, Edholm O, Jahnig F (1997) Molecular dynamics simulations of a fluid bilayer of dipalmitoylphosphatidycholine at full hydration, constant pressure and constant temperature. Biophys J 72:2002–2013

Bernèche S, Roux B (2000) Molecular dynamics of the KcsA K^+ channel in a bilayer membrane. Biophys J 78:2900–2917

Biggin PC, Sansom MSP (2001) Channel gating: twist to open. Curr Biol 11:R364–R366

Biggin PC, Roosild T, Choe S (2000) Potassium channel structure: domain by domain. Curr Opin Struct Biol 10:456–461

Biggin PC, Shrivastava IH, Smith GR, Sansom MSP (2001a) Non-equilibrium molecular dynamics study of KcsA gating. Biophys J 80:514

Biggin PC, Smith GR, Shrivastava IH, Choe S, Sansom MSP (2001b) Potassium and sodium ions in a potassium channel studied by molecular dynamics simulations. Biochim Biophys Acta 1510:1–9

Camino DD, Holmgren M, Liu Y, Yellen G (2000) Blocker protection in the pore of a voltage-gated K^+ channel and its structural implications. Nature 403:321–325

Capener CE, Sansom MSP (2002) MD simulations of a K channel model – sensitivity to changes in ions, waters and membrane environment. J Phys Chem B (in press)

Capener CE, Shrivastava IH, Ranatunga KM, Forrest LR, Smith GR, Sansom MSP (2000) Homology modelling and molecular dynamics simulation studies of an inward rectifier potassium channel. Biophys J 78:2929–2942

Chung SH, Allen TW, Hoyles M, Kuyucak S (1999) Permeation of ions across the potassium channel: Brownian dynamics studies. Biophys J 77:2517–2533

Cortes DM, Cuello LG, Perozo E (2001) Molecular architecture of full-length KcsA: role of cytoplasmic domains in ion permeation and activation gating. J Gen Physiol 117:165–180

Cuello LG, Romero JG, Cortes DM, Perozo E (1998) pH-dependent gating in the *Streptomyces lividans* K^+ channel. Biochemistry 37:3229–3236

Darden T, York D, Pedersen L (1993) Particle mesh Ewald – an N log(N) method for Ewald sums in large systems. J Chem Phys 98:10089–10092

Doyle DA, Cabral JM, Pfuetzner RA, Kuo A, Gulbis JM, Cohen SL, Cahit BT, MacKinnon R (1998) The structure of the potassium channel: molecular basis of K^+ conduction and selectivity. Science 280:69–77

Guidoni L, Torre V, Carloni P (1999) Potassium and sodium binding in the outer mouth of the K^+ channel. Biochemistry 38:8599–8604

Guidoni L, Torre V, Carloni P (2000) Water and potassium dynamics in the KcsA K^+ channel. FEBS Lett 477:37–42

Heginbotham L, LeMasurier M, Kolmakova-Partensky L, Miller C (1999) Single *Streptomyces lividans* K^+ channels: functional asymmetries and sidedness of proton activation. J Gen Physiol 114:551–559

Hess B, Bekker H, Berendsen HJC, Fraaije JGEM (1997) LINCS: a linear constraint solver for molecular simulations. J Comput Chem 18:1463–1472

Hille B (1992) Ionic channels of excitable membranes, 2nd edn. Sinauer, Sunderland, Mass

Hunenberger PH, McCammon JA (1999) Ewald artifacts in computer simulations of ionic solvation and ion-ion interaction. J Chem Phys 110:1856–1872

Im W, Seefeld S, Roux B (2000) Grand canonical Monte Carlo-Brownian dynamics algorithm for simulating ion channels. Biophys J 79:788–801

Jiang YX, MacKinnon R (2000) The barium site in a potassium channel by X-ray crystallography. J Gen Physiol 115:269–272

Kabsch W, Sander C (1983) Dictionary of protein secondary structure: pattern-recognition of hydrogen-bonded and geometrical features. Biopolymers 22:2577–2637

Kraulis PJ (1991) MOLSCRIPT: a program to produce both detailed and schematic plots of protein structures. J Appl Crystallogr 24:946–950

Lindahl E, Edholm O (2000) Mesoscopic undulations and thickness fluctuations in lipid bilayers from molecular dynamics simulations. Biophys J 79:426–433

Luzhkov VB, Åqvist J (2000) A computational study of ion binding and protonation states in the KcsA potassium channel. Biochim Biophys Acta 1481:360–370

MacKinnon R, Cohen SL, Kuo A, Lee A, Chait BT (1998) Structural conservation in prokaryotic and eukaryotic potassium channels. Science 280:106–109

Marrink SJ, Berger O, Tieleman DP, Jahnig F (1998) Adhesion forces of lipids in a phospholipid membrane studied by molecular dynamics simulations. Biophys J 74:931–943

Merritt EA, Bacon DJ (1997) Raster3D: photorealistic molecular graphics. Methods Enzymol 277:505–524

Meuser D, Splitt H, Wagner R, Schrempf H (1999) Exploring the open pore of the potassium channel from *Steptomyces lividans*. FEBS Lett 462:447–452

Meuser D, Splitt H, Wagner R, Schrempf H (2001) Mutations stabilizing an open conformation within the external region of the permeation pathway of the potassium channel KcsA. Eur Biophys J 30:385–391

Minor DL (2001) Potassium channels: life in the post-structural world. Curr Opin Struct Biol 11:408–414

Perozo E, Cortes DM, Cuello LG (1998) Three-dimensional architecture and gating mechanism of a K^+ channel studied by EPR spectroscopy. Nat Struct Biol 5:459–469

Perozo E, Cortes DM, Cuello LG (1999) Structural rearrangements underlying K^+-channel activation gating. Science 285:73–78

Perozo E, Liu YS, Smopornpisut P, Cortes DM, Cuello LG (2000) A structural perspective of activation gating in K^+ channels. J Gen Physiol 116:5a

Ranatunga KM, Shrivastava IH, Smith GR, Sansom MSP (2001a) Sidechain ionisation states in a potassium channel. Biophys J 80:1210–1219

Ranatunga KM, Smith GR, Law RJ, Sansom MSP (2001b) Electrostatics and molecular dynamics of a homology model of the *Shaker* K^+ channel pore. Eur Biophys J 30:295–303

Roux B (1999) Statistical mechanical equilibrium theory of selective ion channels. Biophys J 77:139–153

Roux B, MacKinnon R (1999) The cavity and pore helices in the KcsA K^+ channel: electrostatic stabilization of monovalent cations. Science 285:100–102

Roux B, Berneche S, Im W (2000) Ion channels, permeation and electrostatics: insight into the function of KcsA. Biochemistry 39:13295–13306

Sansom MSP, Weinstein H (2000) Hinges, swivels and switches: the role of prolines in signalling via transmembrane α-helices. Trends Pharm Sci 21:445–451

Sansom MSP, Shrivastava IH, Ranatunga KM, Smith GR (2000) Simulations of ion channels – watching ions and water move. Trends Biochem Sci 25:368–374

Schirmer T, Phale PS (1999) Brownian dynamics simulation of ion flow through porin channels. J Mol Biol 294:1159–1167

Schnitzer J, Mashl RJ, Subramaniam S, Jakobsson E (2000) KcsA potassium channel: calculation of pore electrostatic potential from the 3-dimension structure and of potassium ion flux by one-dimensional Brownian dynamics. Biophys J 78:1960Pos

Schrempf H, Schmidt O, Kummerlein R, Hinnah S, Muller D, Betzler M, Steinkamp T, Wagner R (1995) A prokaryotic potassium-ion channel with 2 predicted transmembrane segments from *Steptomyces lividans*. EMBO J 14:5170–5178

Shrivastava IH, Sansom MSP (2000) Simulations of ion permeation through a potassium channel: molecular dynamics of KcsA in a phospholipid bilayer. Biophys J 78:557–570

Shrivastava IH, Capener C, Forrest LR, Sansom MSP (2000) Structure and dynamics of K^+ channel pore-lining helices: a comparative simulation study. Biophys J 78:79–92

Shrivastava IH, Biggin PC, Tieleman DP, Sansom MSP (2002) K^+ vs. Na^+ ions in a K channel selectivity filter: a simulation study. Biophys J (in press)

Smart OS, Goodfellow JM, Wallace BA (1993) The pore dimensions of gramicidin A. Biophys J 65:2455–2460

Smart OS, Breed J, Smith GR, Sansom MSP (1997) A novel method for structure-based prediction of ion channel conductance properties. Biophys J 72:1109–1126

Splitt H, Meuser D, Borovok I, Betzler M, Schrempf H (2000) Pore mutations affecting tetrameric assembly and functioning of the potassium channel from *Steptomyces lividans*. FEBS Lett 472:83–87

Straatsma TP, Berendsen HJC (1988) Free-energy of ionic hydration – analysis of a thermodynamic integration technique to evaluate free-energy differences by molecular-dynamics simulations. J Chem Phys 89:5876–5886

Sukharev S, Betanzos M, Chiang CS, Guy HR (2001) The gating mechanism of the large mechanosensitive channel MscL. Nature 409:720–724

Tieleman DP, Berendsen HJC (1996) Molecular dynamics simulations of a fully hydrated dipalmitoylphosphatidycholine bilayer with different macroscopic boundary conditions and parameters. J Chem Phys 105:4871–4880

Tieleman DP, Biggin PC, Smith GR, Sansom MSP (2001a) Simulation approaches to ion channel structure-function relationships. Quart Rev Biophys 34:473–561

Tieleman DP, Shrivastava IH, Ulmschneider MB, Sansom MSP (2001b) Proline-induced hinges in transmembrane helices: possible roles in ion channel gating. Proteins Struct Funct Genet 44:63–72

Weber W, Hunenberger PH, McCammon JA (2000) Molecular dynamics simulations of a polyalanine octapeptide under Ewald boundary conditions: influence of artificial periodicity on peptide conformation. J Phys Chem B 104:3668–3675

Zhou M, Morais-Cabral JH, Mann S, MacKinnon R (2001) Potassium channel receptor site for the inactivation gate and quaternary amine inhibitors. Nature 411:657–661